Rasmussen, H. (1986b) *N. Engl. J. Med. 314*, 1164-1170.
Richardson, J. S., & Richardson, D. C. (1988) *Science 240*, 1648-1652.
Seamon, K. B., & Kretsinger, R. H. (1983) Calcium Binding Proteins, *Met. Ions Biol. 6*, 1-52.
Szebenyi, D. M. E., & Moffat, K. (1986) *J. Biol. Chem. 261*, 8761-8777.
Szebenyi, D. M. E., Obendorf, S. K., & Moffat, K. (1981) *Nature 294*, 327-332.
Wagner, G. (1983) *J. Magn. Reson. 55*, 151-156.
Wendt, B., Hofmann, T., Martin, S. T., Bayley, P., Brodin, P., Grundström, T., Thulin, E., Linse, S., & Forsén, S. (1988) *Eur. J. Biochem. 175*, 439-445.
Wüthrich, K. (1983) *Biopolymers 22*, 131-138.
Wüthrich, K. (1986) *NMR of Proteins and Nucleic Acids*, Wiley, New York.
Wüthrich, K., Billeter, M., & Braun, W. (1984) *J. Mol. Biol. 180*, 715-740.

Assignment of the Proton NMR Spectrum of Reduced and Oxidized Thioredoxin: Sequence-Specific Assignments, Secondary Structure, and Global Fold†

H. Jane Dyson,‡ Arne Holmgren,§ and Peter E. Wright*,‡

Department of Molecular Biology, Research Institute of Scripps Clinic, La Jolla, California 92037, and Department of Physiological Chemistry, Karolinska Institutet, S-10401 Stockholm, Sweden

Received February 6, 1989; Revised Manuscript Received May 5, 1989

ABSTRACT: Complete proton assignments are reported for the ^{1}H nuclear magnetic resonance (NMR) spectrum of *Escherichia coli* thioredoxin in the oxidized (with active-site disulfide bridge) and reduced (with two sulfhydryl groups) states. The assignments were obtained by using an integrated assignment strategy in which spin systems were identified from a combination of relayed and multiple quantum NMR techniques prior to sequential assignment. Elements of secondary structure were identified in each protein from characteristic nuclear Overhauser effects (NOE), coupling constants, and slowly exchanging amide protons. In both oxidized and reduced thioredoxin, approximately 33% of the 108 amino acid residues participate in a β-sheet containing four major strands (three antiparallel and one parallel). A further short β-strand is connected in a parallel fashion at the N-terminal end of the sheet. Two of the antiparallel β-strands are connected by a 7-residue β-bulge loop. Three helical segments, also containing approximately 33% of the amino acid residues, are well-defined in both oxidized and reduced thioredoxin. The remaining third of the molecule apparently consists of reverse turns and loops with little defined secondary structure. The global folds of oxidized and reduced thioredoxin are shown to be essentially identical. Both NOE connectivities and chemical shift values for the two proteins are very similar, except in the immediate vicinity of the active site where significant variations in the chemical shift indicate subtle conformational changes. While the overall fold of oxidized thioredoxin is the same in solution and in the crystalline state, some small differences in local conformation are apparent.

Thioredoxin is a ubiquitous protein (M_r = 11 700) with many functions, particularly in thiol-dependent redox reactions [for a review, see Holmgren (1985)]. The active site of thioredoxin, Cys-Gly-Pro-Cys, contains a disulfide in the oxidized form. This is usually reduced by NADPH and the FAD-containing enzyme thioredoxin reductase to a dithiol in the reduced form of thioredoxin. Reduced thioredoxin is a powerful general protein disulfide reductase and also a hydrogen donor for ribonucleotide reductase, methionine sulfoxide reductases, and sulfate reductase. In addition, the reduced form of *Escherichia coli* thioredoxin is essential for phage T7 DNA replication as a subunit of T7 DNA polymerase and for assembly of filamentous phages f1 and M13.

The 108-residue amino acid sequence of *E. coli* thioredoxin (Holmgren, 1968) and the nucleotide sequence of the corresponding *trxA* gene (Höög et al., 1984; Lim et al., 1985) are known. The three-dimensional structure of oxidized thioredoxin has been solved by X-ray crystallography at 2.8-Å resolution (Holmgren et al., 1975). The active-site disulfide (between Cys 32 and Cys 35) is located in a protrusion of the molecule at the end of a β-strand and immediately followed by an α-helix. The X-ray structure of oxidized thioredoxin shows about 75% of the molecule in well-defined secondary structure elements, including four helices and five strands of β-sheet. Thioredoxin has been isolated from many different organisms and, for example, the primary structures of about 10 prokaryotic thioredoxins show about 50% positional identity to *E. coli* thioredoxin [for a review, see Gleason and Holmgren (1988)], consistent with a protein ancient on the evolutionary time scale, with a conserved global fold.

The three-dimensional structure of reduced thioredoxin is not known, since it has not been possible to crystallize the protein in this state. Previous spectroscopic studies (Stryer et al., 1967; Holmgren, 1972; Holmgren & Roberts, 1976) suggest that no gross structural changes occur on reduction of thioredoxin. Functional data show that enzymes such as thioredoxin reductase and ribonucleotide reductase discriminate between oxidized and reduced thioredoxin. Furthermore, only the reduced conformation of thioredoxin is able to activate gene 5 protein of phage T7 DNA polymerase (Mark &

†Supported by Grant GM 36643 from the National Institutes of Health and Grant 13x - 3529 from the Swedish Medical Research Council and by the Karolinska Institutet.
‡Research Institute of Scripps Clinic.
§Karolinska Institutet.

0006-2960/89/0428-7074$01.50/0

Richardson, 1976) or function in the assembly of f1 or M13 phage (Huber et al., 1986; Russel & Model, 1985, 1986).

We have previously reported preliminary results from a comparison of the two-dimensional ^1H NMR[1] spectra of reduced and oxidized thioredoxin (Dyson et al., 1988a). Significant differences were observed between the two forms in the chemical shifts of amino acid residues in the active site and in some distant parts of the primary structure known from the X-ray crystal structure to be close to the active site in the intact protein. These residues form a hydrophobic molecular surface proposed to be involved in binding of other proteins (Eklund et al., 1984).

We here report complete proton assignments for the ^1H NMR spectrum of *E. coli* thioredoxin in both the reduced and oxidized forms. These results are at present being used to generate solution structures of the proteins by distance geometry calculations. LeMaster and Richards (1988) have also reported backbone sequential assignments for oxidized thioredoxin, using random fractional deuteration to simplify the assignment procedure.

Experimental Procedures

Protein Preparation. Thioredoxin for the present studies was prepared from the overproducing strain SK3981, which contains the plasmid pBHK8 with the *trxA* gene ligated into pBR325 (Lunn et al., 1984; Höög et al., 1984). Cells were grown in an automatic 100-L fermentor with 100 μg/mL of ampicillin in Frazer medium with glycerol as the carbon source. The cells were harvested in late stationary phase (24 h after start) by a Sharples centrifuge (yield 4 kg of packed cells) and were stored at −70 °C after disintegration with an X-press at −20 °C (Holmgren & Reichard, 1967). All preparative operations were carried out at +4 °C. Centrifugations were at 10000*g* in a Sorvall RC5 centrifuge. Frozen cells (200 g) were homogenized with a Turmix in 1000 mL of 50 mM Tris-HCl and 3 mM EDTA, pH 7.5, containing 1 mM PMSF, and a crude extract was obtained by centrifugation for 60 min. To the crude extract was slowly added $^1/_{10}$ volume of freshly prepared 7% streptomycin sulfate followed by gentle stirring on ice for 30 min. Precipitated nucleic acids were removed by centrifugation for 30 min, and the supernatant solution was brought to 85% saturation with solid ammonium sulfate. Precipitated protein was dissolved in 150 mL of 20 mM potassium phosphate, pH 7.3, and 1 mM EDTA, dialyzed extensively, and applied to a column of D-32 cellulose (6 × 15 cm) (Whatman) that was eluted with a 6-L gradient of 20 mM potassium phosphate, pH 7.3, 3 mM EDTA, and 350 mM potassium phosphate, pH 7.3, 3 mM EDTA. Protein was determined by absorbance at 280 nm and thioredoxin activity with the DTNB assay using thioredoxin reductase (Holmgren & Reichard, 1967). Thioredoxin-containing fractions were pooled and concentrated by ultrafiltration with Diaflo membranes and applied to a Sephadex G-50 column (6 × 125 cm) equilibrated with 50 mM Tris-HCl, pH 7.5, and 1 mM EDTA. Active fractions were concentrated by ultrafiltration, and the yield of thioredoxin after this step was about 1000 mg of protein with better than 95% purity as estimated by SDS–polyacrylamide gel electrophoresis or measurement of the disulfide content by NADPH oxidation (Holmgren & Reichard, 1967). The final step consisted of a buffer exchange to 0.07 M acetic acid and 0.04 M ammonia, pH 4.79, on a Sephadex G-25 column and isocratic chromatography on a column of DE-32 cellulose (4 × 20 cm) equilibrated with this buffer (Holmgren & Reichard, 1967). Thioredoxin elutes after about 4 column volumes. Between 5 and 10% of the protein remained bound on the column and appears to represent deamidated but active forms (Holmgren, 1968), some aggregates, and minor impurities. The pH of the active fractions was immediately adjusted to 8.0 with 1 M NH_3 and the material concentrated by ultrafiltration to about 100 mg/mL and stored at −70 °C. Protein concentration was determined at 280 nm by using a molar extinction coefficient of 13 700 cm^{-1} M^{-1} (Holmgren & Reichard, 1967).

Thioredoxin solutions were prepared for NMR measurements by buffer exchange on a small column of Sephadex G-25 equilibrated with 0.1 M potassium phosphate of the desired pH in either ^2H_2O or 90% ^1H_2O/10% ^2H_2O. Concentrations were adjusted to about 4 mM by ultrafiltration. Thioredoxin was reduced by addition of 1 M freshly prepared dithiothreitol (DTT) in the appropriate buffer to a final concentration of 10 mM. The protein and DTT solutions were equilibrated under argon, and the NMR tube was sealed with a rubber septum under argon.

In many cases, the protein was passed through a Sephadex G-25 column after reduction to remove DTT. The protein was found to be stable in the reduced state in the absence of DTT. Unless otherwise stated, thioredoxin solutions were at pH 5.70, 0.1 M potassium phosphate buffer in 90% ^1H_2O/10% ^2H_2O or in ^2H_2O (the pH represents an uncorrected meter reading).

NMR Measurements. Spectra were obtained on a Bruker AM500 spectrometer equipped with digital phase-shifting hardware. Spectra were recorded at 298, 308, and 328 K and were referenced to internal dioxan (3.75 ppm downfield from DSS). Standard methods were used to obtain 2QF-COSY (Rance et al., 1983), R-COSY (Eich et al., 1982), TOCSY (Bax & Davis, 1985; Rance, 1987), double quantum (Braunschweiler et al., 1986; Rance & Wright, 1986), and NOESY (Jeener et al., 1979) spectra for both oxidized and reduced thioredoxin in 90% ^1H_2O/10% ^2H_2O. The R-COSY spectra were acquired with mixing times of 40 and 80 ms (Chazin & Wüthrich, 1987), the 2Q spectra with an excitation period of 22 ms, and the TOCSY spectra with a spin-lock period of 80 ms. NOESY spectra were acquired with mixing times of 30, 50, 80, 120, and 150 ms for both oxidized and reduced thioredoxin in 90% ^1H_2O/10% ^2H_2O. NOESY spectra were also acquired for both proteins with a mixing time of 150 ms and with the observe pulse replaced by a $45°_{(x)}$–τ–$45°_{(-x)}$ sequence (Clore & Gronenborn, 1983). Spectra acquired for both oxidized and reduced thioredoxin in ^2H_2O solution included 2QF-COSY, 3QF-COSY (Rance & Wright, 1986), TOCSY with a spin-lock period of 80 ms, 2Q spectra with an excitation period of 22 ms, 3Q spectra with an excitation period of 22 ms, and NOESY spectra with a mixing time of 150 ms.

Spectra were acquired with 4096 complex data points, and the spectral width was commonly 7000 Hz for spectra in 90% ^1H_2O/10% ^2H_2O (digital resolution 3.4 Hz/point) and 5200 Hz for spectra in ^2H_2O (digital resolution 2.5 Hz/point). Quadrature detection in ω_1 was achieved by using time proportional phase incrementation (Drobny et al., 1979); 400–700 t_1 points were acquired for two-dimensional spectra. In some cases spectra were folded in ω_1 for better digital resolution.

[1] Abbreviations: NMR, nuclear magnetic resonance; DTNB, 5,5′-dithiobis(2-nitrobenzoic acid); DTT, dithiothreitol; PMSF, phenylmethanesulfonyl fluoride; COSY, two-dimensional correlated spectroscopy; TOCSY, two-dimensional total correlation spectroscopy; R-COSY, two-dimensional relay spectroscopy; MQ, 2Q, etc., multiple, double, etc., quantum spectroscopy; MQF-COSY, multiple quantum filtered COSY spectroscopy; NOESY, two-dimensional nuclear Overhauser effect spectroscopy.

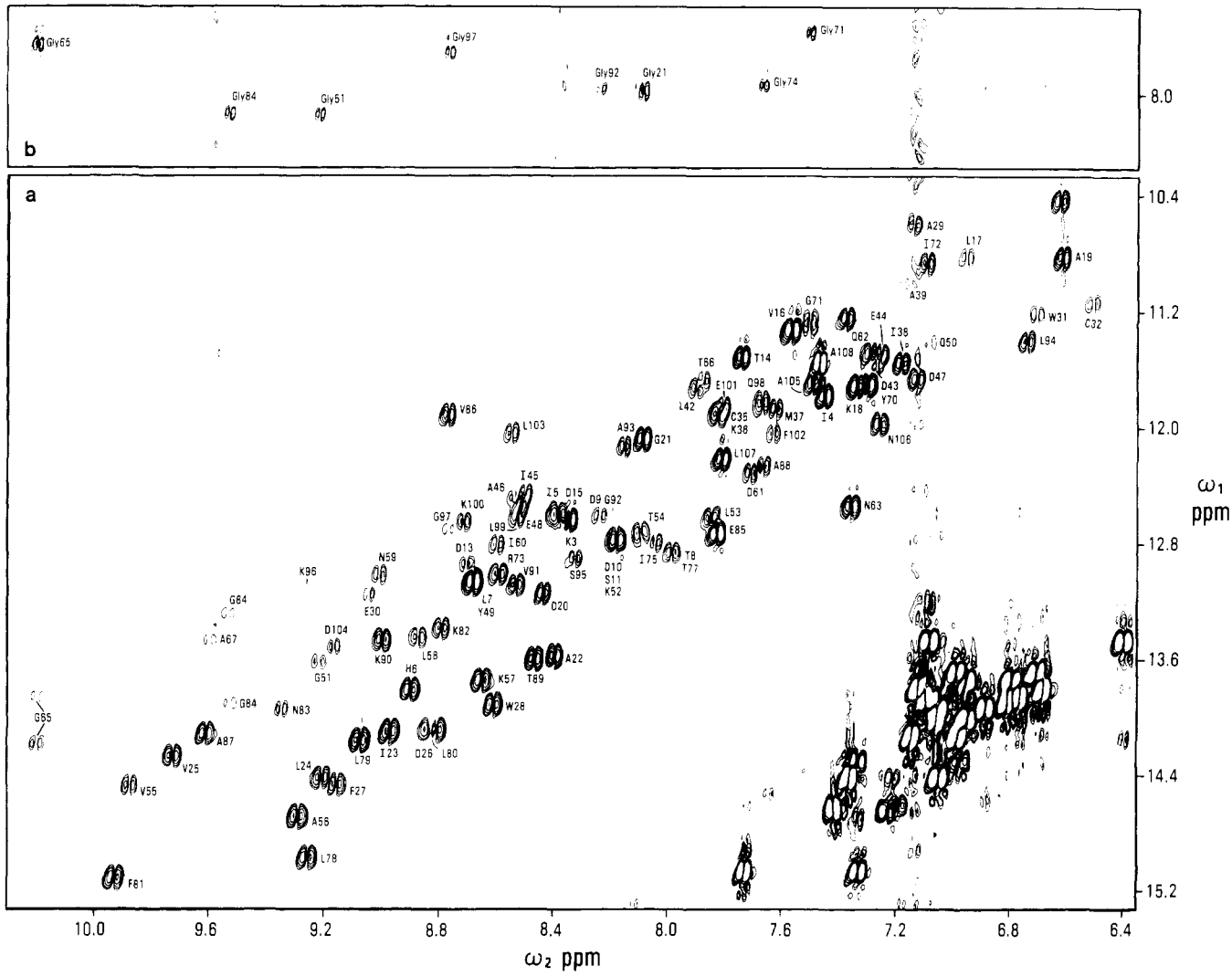

FIGURE 1: Portion of a 500-MHz phase-sensitive double quantum spectrum of reduced thioredoxin in 90% ^1H_2O/10% ^2H_2O, pH 5.70. The spectrum was acquired with quadrature detection in ω_1 (Drobny et al., 1979) and without solvent suppression during the excitation period. (a) NH–C$^\alpha$H and aromatic portions; (b) region showing remote peaks at $\omega_2 = \omega_{NH}$, $\omega_1 = \omega_\alpha + \omega_{\alpha'}$ for glycine residues.

COSY spectra contained more t_1 points, for a digital resolution of about 7.0 Hz/point in ω_1. For NOESY and TOCSY experiments, fewer t_1 points (400–500) were necessary.

Two-dimensional spectra were processed by using a SUN 3 workstation fitted with a Sky Warrior array processor, with software provided by Dr. D. Hare and modified by Dr. J. Sayre. Phase-shifted sine bell window functions were used in both dimensions. For NOESY, TOCSY, and 2Q spectra in 90% ^1H_2O/10% ^2H_2O, considerable improvement was obtained by base-line correction and suppression of t_1 ridges (Otting et al., 1986).

The slowly exchanging amide protons indicated in Figures 3 and 5 for reduced and oxidized thioredoxin, respectively, were identified from COSY or NOESY spectra acquired at 308 K within 24 h of exchanging the protein into ^2H_2O at pH 5.7. The magnitude of $^3J_{HN\alpha}$ coupling constants was estimated from the peak-to-peak multiplet separation in cross sections of COSY spectra (Marion & Wüthrich, 1983) that had been processed with zero filling to give high digital resolution (0.8 Hz/point). The large line width of many of the amide proton resonances of thioredoxin (>10 Hz) means that many of the smaller coupling constants could not be determined directly from the COSY cross peaks in a straightforward way (Neuhaus et al., 1985). Estimates of the coupling constant in many of these cases could be made by computer simulation on the basis of line widths in the NOESY spectra and the degree of attenuation of the COSY cross-peak intensity. This method will be described in detail elsewhere.

RESULTS

Proton resonance assignments were made by using a strategy (Chazin & Wright, 1987) that has been successfully used for the assignment of French bean plastocyanin (Chazin et al., 1988a; Chazin & Wright, 1988) and C3a (Chazin et al., 1988b). In this strategy, spin system assignments are first obtained as completely as possible by utilizing the favorable dispersion of the amide proton resonances and relaying magnetization from the side chain to the backbone NH proton resonance. Most experiments are carried out with protein solutions in 90% ^1H_2O/10% ^2H_2O. Not all NH–C$^\alpha$H cross peaks appear in the COSY spectrum of thioredoxin as a result of overlap of some C$^\alpha$H resonances with that of H_2O, relatively fast exchange of some NH protons with H_2O, and small $^3J_{HN\alpha}$ coupling constants. Further NH–C$^\alpha$H cross peaks could be identified from 2Q, R-COSY, and TOCSY spectra and by varying experimental conditions such as temperature and pH. The most complete set of NH–C$^\alpha$H cross peaks was obtained by using a 2Q spectrum, shown for reduced thioredoxin in Figure 1 and for the oxidized protein in Figure 1S. Assignments were facilitated by using both oxidation states of thioredoxin; ambiguities due to cross-peak overlap and resonance degeneracies in the spectra of one oxidation state often

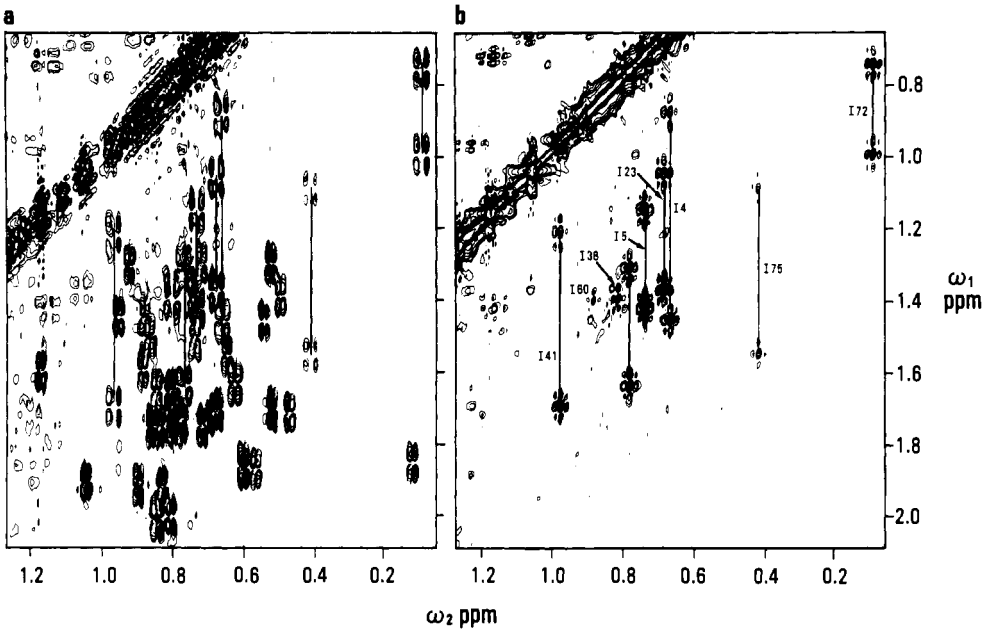

FIGURE 2: (a) Portion of a 500-MHz phase-sensitive 2QF-COSY spectrum of reduced thioredoxin in ^2H_2O at 308 K, pH 5.70, showing the $C^\beta H$–$C^\gamma H_3$ and $C^\beta H$–$C^{\gamma'} H_3$ cross peaks of the valine residues, the $C^\gamma H$–$C^\delta H_3$ and $C^\gamma H$–$C^{\delta'} H_3$ cross peaks of the leucine residues, and the $C^\beta H$–$C^\gamma H_3$, $C^\gamma H$–$C^\delta H_3$, and $C^{\gamma'} H$–$C^\delta H_3$ cross peaks of the isoleucine residues. Both positive and negative levels are shown. (b) Portion of the same region of a 500-MHz phase-sensitive 3QF-COSY spectrum of reduced thioredoxin in ^2H_2O at 308 K. Only the $C^\gamma H$–$C^\delta H_3$ and $C^{\gamma'} H$–$C^\delta H_3$ cross peaks of the isoleucine residues appear. Both positive and negative levels are shown.

do not occur in the other, in spite of the overall similarity of the spectra of the two proteins (Dyson et al., 1988a).

Spin System Assignments. An overview of the strategy for spin system assignments is given in this section. Details of individual cases where difficulty was experienced are given in the supplementary material, together with a summary of the scalar connectivities observed for all residues (Table IS).

Glycine residues were assigned readily by observation of unique remote peaks at $\omega_2 = \omega_{NH}$, $\omega_1 = \omega_\alpha + \omega_{\alpha'}$ in double quantum spectra recorded in 90% ^1H_2O/10% ^2H_2O (Figure 1). All of the direct $C^\alpha H/C^{\alpha'} H$ connectivities were observed in the 2QF-COSY and 2Q spectra with the exception of Gly 21, where the $C^\alpha H$ resonances are degenerate for both the oxidized and reduced protein. For Gly 71 the two $C^\alpha H$ chemical shifts are too close together to observe clear cross peaks in the 2QF-COSY spectra, but cross peaks could be resolved in 2Q spectra. All glycine assignments were straightforward for both oxidation states, with the single exception of Gly 33. Further details of the assignment of the resonances of this important active-site residue are given in a later section.

With one exception, alanine and threonine residues were identified readily. In both oxidized and reduced thioredoxin, the $C^\alpha H$ and $C^\beta H$ resonances of Thr 8 are nearly degenerate and lie under the H_2O resonance at 308 K. These resonances were identified in spectra obtained at 298 and 328 K and in spectra in ^2H_2O.

For each of the spin systems of valine, leucine, and isoleucine, scalar connectivities can usually be established for the NH–$C^\alpha H$–$C^\beta H$ and for the $C^\beta H$–$C^\gamma H_3$ (Val, Ile) and $C^\gamma H$–$C^\delta H_3$ (Leu, Ile) fragments of the spin system. The methyl resonances of these residues are often relatively well resolved and not complicated by multiple couplings. The scalar connectivities thus give two spin subsystems: the problem for assignment of the complete spin systems is the connection of the two subsystems. In oxidized and reduced thioredoxin, the task of assigning these aliphatic side chains was complicated by the large numbers of them (5 valines, 13 leucines, and 9 isoleucines), which resulted in extensive overlap in the methyl group region (Figure 2). Nevertheless, complete assignment was achieved. Assignments were made primarily by using TOCSY spectra but were confirmed in all cases by multiple quantum spectroscopy. The 2Q spectrum in ^2H_2O was particularly useful for confirmation of both $C^\beta H$ assignments of the leucine residues. In general, only one of the two possible $C^\alpha H$–$C^\beta H$ cross peaks was observed at $\omega_2 = \omega_\alpha$, but the other $C^\beta H$ assignment could generally be obtained from the remote peak at $\omega_2 = \omega_\alpha$, $\omega_1 = \omega_\beta + \omega_{\beta'}$.

Identification of all of the valine spin systems was relatively straightforward with R-COSY and TOCSY spectra. Isoleucine assignments were more problematical due to the overlap and broadness of the resonances in both oxidized and reduced thioredoxin. The $C^\beta H$ and $C^\gamma H_3$ resonances of the isoleucine residues could be readily assigned in most cases from cross peaks at the NH frequency in R-COSY and TOCSY spectra in 90% ^1H_2O/10% ^2H_2O. However, no TOCSY cross peaks were generally observed between the NH resonance and the $C^\gamma H_2$ or $C^\delta H_3$ resonances of the isoleucine residues. COSY connectivities between the $C^\delta H_3$ triplet and the two $C^\gamma H$ resonances were established for all but two of the isoleucines. Of particular use in identifying $C^\gamma H_2$ and $C^\delta H_3$ cross peaks in crowded spectra are 3Q and 3QF-COSY spectra (Chazin et al., 1988a; Rance et al., 1989). The 3QF-COSY spectrum of reduced thioredoxin (Figure 2) indicates that the two $C^\gamma H$ resonances of Ile 38 and Ile 60 are virtually degenerate in each case. This is confirmed in the 3Q spectrum. Connection of the NH–$C^\alpha H$–$C^\beta H$–$C^\gamma H_3$ and $C^\gamma H$–$C^{\gamma'} H$–$C^\delta H_3$ spin subsystems of all but two of the isoleucines in both reduced and oxidized thioredoxin was made by using a TOCSY spectrum in ^2H_2O. Assignment of the last two isoleucines, Ile 23 and Ile 75, was not straightforward; details are given in the supplementary material.

The connections between the NH–$C^\alpha H$–$C^\beta H_2$ and $C^\gamma H$–$C^\delta H_3$–$C^{\delta'} H_3$ subsystems for most leucine residues were also made by using TOCSY spectra. The large number of leucines (13) made R-COSY experiments less useful for assignment, since many of the $C^\beta H_2$ and $C^\gamma H$ resonances were badly overlapped. The majority of the spin systems were identified

by using TOCSY spectra in ^2H_2O through observation of cross peaks between the $C^{\alpha}H$ and the $C^{\delta}H_3$ resonances. The TOCSY spectra in 90% ^1H_2O/10% ^2H_2O did not in general show cross peaks between NH resonances and the leucine $C^{\delta}H_3$ resonances. Only two leucine spin systems, Leu 58 and Leu 7, could not be assigned directly from the TOCSY spectra in ^2H_2O (see supplementary material).

The AMX spin systems of the $C^{\alpha}H$–$C^{\beta}H_2$ portions of Asp, Asn, Phe, Tyr, Ser, Cys, Trp, and His were assigned by using relayed magnetization-transfer techniques such as R-COSY and TOCSY for protein in 90% ^1H_2O/10% ^2H_2O solutions. In all cases, assignments were confirmed by using multiple quantum spectra. 2Q spectra are particularly important in this regard since the remote peaks at $\omega_2 = \omega_{\alpha}$, $\omega_1 = \omega_{\beta} + \omega_{\beta'}$ usually occur in uncrowded regions of the spectrum. The aromatic side-chain resonances of the Phe, Tyr, Trp, and His residues were readily assigned by using 2QF-COSY spectra, with confirmation from 2Q spectra in cases of overlap. Weak COSY and 2Q cross peaks were observed for the $C^{\delta}H$–$C^{\epsilon}H$ connectivity of the single histidine. All of the Phe and Tyr residues give rise to AA′BB′C and AA′BB′ spin systems, indicating that all the aromatic rings flip rapidly on the NMR time scale. Assignment of the relevant AMX spin systems of the aromatic amino acids was made on the basis of strong NOESY cross peaks between the $C^{\delta}H$ and the $C^{\beta}H$ resonances. Often, confirmatory NOEs were observed between the $C^{\delta}H$ resonance and the $C^{\alpha}H$ or NH resonances.

Certain of the three-spin spin systems were difficult to assign for both oxidized and reduced thioredoxin. These included Asp 9, Phe 12, Ser 11, Ser 95, and the two cysteines (see supplementary material for details). The spin systems of Ser 1 and Asp 2 were identified by elimination. No amide proton resonance could be observed for Asp 2 in the spectrum of oxidized or reduced thioredoxin, and Ser 1 does not have an amide proton. The Ser 1 $C^{\alpha}H$, $C^{\beta}H$, and $C^{\beta'}H$ resonances were assigned to a spin system characterized by sharp lines and observed in all spectra at 4.19, 3.90, and 4.05 ppm. The chemical shifts are typical for a serine, and the narrow lines are consistent with the position of Ser 1 at the end of the polypeptide chain.

The glutamic acid, glutamine, and methionine residues were assigned without difficulty from COSY, R-COSY, and TOCSY Spectra. In general, one of the $C^{\beta}H$ protons could be obtained from the 2QF-COSY spectrum from its cross peak to the $C^{\alpha}H$ proton. The other $C^{\beta}H$ resonance was obtained from R-COSY or 2Q spectra or directly from the 3QF-COSY spectrum. The $C^{\gamma}H$ resonances were assigned usually by TOCSY, on the basis of connectivities to the NH in the TOCSY spectrum in 90% ^1H_2O/10% ^2H_2O or to the $C^{\alpha}H$ in the TOCSY in ^2H_2O.

Lysine and arginine were assigned principally from TOCSY and multiple quantum spectra as has been described elsewhere (Chazin et al., 1987). Assignment of the single arginine residue was relatively straightforward. Assignment of the 10 lysines was more difficult, mainly because of overlap of the $C^{\epsilon}H_2$ resonances. The $C^{\epsilon}H_2$ and $C^{\delta}H_2$ resonances could, however, be identified from the double quantum spectrum, where the remote peaks on the $C^{\epsilon}H_2$ resonances at $\omega_1 = \omega_{\delta} + \omega_{\delta'}$ are fairly well resolved. The assignments of the lysine residues were completed by matching spin subsystems based on the $C^{\epsilon}H_2$ resonances and on the $C^{\alpha}H$ resonances in TOCSY spectra and were finally checked by using multiple quantum spectra.

Of all of the amino acids, prolines are the most difficult to assign since they have no NH proton. Identification of the $C^{\delta}H$–$C^{\delta'}H$ cross peaks of prolines was usually straightforward by using 2Q, 2QF-, and 3QF-COSY spectra, but $C^{\alpha}H$ resonances sometimes presented difficulties. For this reason, assignment of the prolines was largely deferred until sequential assignment of the other residues had been completed, whereupon it was possible to use sequential NOE connectivities from neighboring residues to identify the $C^{\alpha}H$ and $C^{\delta}H_2$ resonances. Spin subsystems based on these resonances were identified in the TOCSY spectrum in ^2H_2O and were used to complete the assignment of the proline spin systems as described by Chazin et al. (1988a).

Completion of the assignments relied upon the use of several types of spectroscopy for the identification of elusive resonances. Of particular importance in establishing complete spin system assignments were TOCSY, 2Q, and 3QF-COSY spectra in ^2H_2O, which allowed the identification of, for example, both $C^{\beta}H$ protons of the leucine residues, the majority of the lysine resonances, and some of the more difficult three-spin, proline and isoleucine spin systems. The proton assignments for reduced and oxidized thioredoxin are summarized in Tables I and II, respectively.

Sequential Assignments. Assignment of individual amino acid spin systems to their correct position in the sequence was achieved by using the sequential assignment procedure of Billeter et al. (1982). For most amino acids the sequential connectivities were straightforward, and either $d_{\alpha N}(i, i + 1)$ NOE connectivities (for extended-chain or β-sheet conformations) or $d_{NN}(i, i + 1)$ connectivites (for helical conformations) were observed. Difficulties were sometimes encountered through overlap of $C^{\alpha}H$ or NH resonances of adjacent amino acids. This could to some extent be relieved by observations at various temperatures and pHs and by comparison of the oxidized and reduced forms.

A summary of the observed interresidue sequential NOE connectivities for reduced thioredoxin is shown in Figure 3. Strong or medium sequential $d_{\alpha N}(i, i + 1)$ NOE connectivities are observed for the residues between Asp 2 and Thr 8, between Lys 18 and Glu 30, between Leu 53 and Ile 60, between Thr 77 and Gly 84, and between Ala 88 and Val 91 (Figure 4), suggesting the presence of β-structure. (A set of figures establishing the β-strand connectivities in oxidized thioredoxin are given in the supplementary material, Figure 2S.) Changes of temperature or the use of NOESY spectra for which composite pulses were used for water suppression confirmed the presence of sequential NOE peaks [and $d_{N\alpha}(i, i)$ peaks] that were obscured by the water resonance at 308 K, the temperature at which most spectra were acquired. For the oxidized protein (Figure 5), the locations of the β-strands, deduced from the $d_{\alpha N}(i, i + 1)$ NOE connectivities, were very similar to those seen for reduced thioredoxin between Asp 2 and Thr 8, between Lys 18 and Glu 30, between Leu 53 and Ile 60, between Thr 77 and Asn 83, and between Ala 88 and Val 91. Figures 3 and 5 also show the locations of slowly exchanging amide protons and residues that have large values of $^3J_{HN\alpha}$ coupling constants.

Amino acid residues in helices were more difficult to assign, mainly because of overlap of the NH resonances of adjacent amino acids. A helical segment from Ser 11 to Ala 19 was well-defined for both oxidized and reduced thioredoxin by sequential d_{NN} (Figure 6) and $d_{\beta N}(i, i + 1)$ connectivities, as well as by $d_{\alpha N}(i, i + 3)$ and $d_{\alpha\beta}(i, i + 3)$ NOEs. Similarly, a helix at the C-terminal end of the molecule, between Lys 96 and Ala 108, is well-defined (Figure 6). It was difficult to make sequential assignments for the helix immediately following the active site, mainly because several adjacent

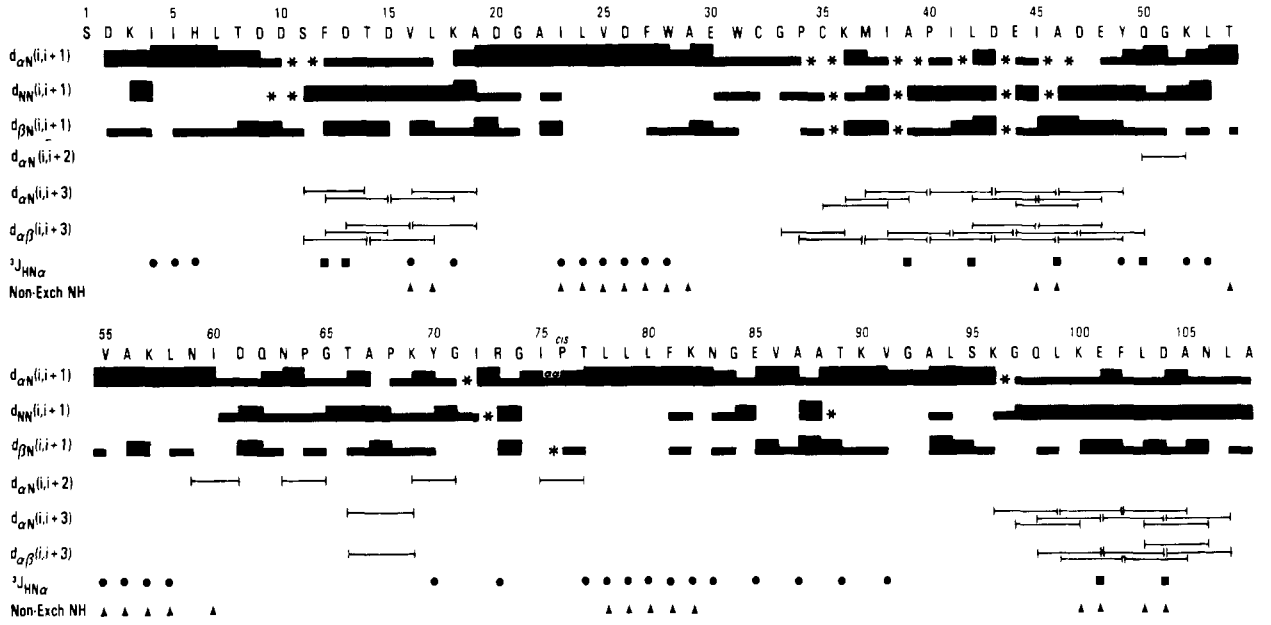

FIGURE 3: Summary of sequential connectivities for reduced thioredoxin. The majority of the data were accumulated at 308 K, pH 5.7, but the diagram includes information from spectra obtained at other temperatures and pHs. Connectivities that were obscured by resonance overlap are labeled with an asterisk. Values of $^3J_{HN\alpha}$ are classified as small (≤6 Hz) or large (≥9 Hz) as indicated by solid squares and circles, respectively. Backbone amide protons that exchange slowly are indicated with a triangle. Note that $d_{\alpha\delta}$, $d_{N\delta}$, etc. connectivities for proline are included as $d_{\alpha N}$, d_{NN} connectivities. The $d_{\alpha\alpha}$ connectivity between Ile 75 and *cis*-Pro 76 is shown as a $d_{\alpha N}$ connectivity.

residues have overlapped NH and C$^\alpha$H resonances. These include, in both oxidation states, Ile 38 and Ala 39 (overlapped NH), Ile 41 and Leu 42 (overlapped C$^\alpha$H), Asp 43 and Glu 44 (overlapped NH and C$^\alpha$H), and Ile 45 and Ala 46 (very close NH and C$^\alpha$H resonances). In addition, for the reduced protein, Cys 35 and Lys 36 have virtually identical NH and C$^\alpha$H resonances in marked contrast to the oxidized protein, where they are well separated and where there is a clear d_{NN} NOE connectivity (Figure 7). That there are indeed two peaks at the K36, C35 cross-peak position is shown by COSY spectra of the reduced protein under various conditions of pH and temperature, when two NH–C$^\alpha$H cross peaks are revealed at this position due to slight shifts in the NH chemical shifts of the two amino acid residues. Pro 40 is located in the helix by NOE connectivities between the C$^\delta$H resonances of the proline and the NH resonances of Ala 39 and Ile 41. For the helix between Cys 35 and Tyr 49 in both oxidized and reduced thioredoxin, an extensive set of $d_{\alpha\beta}(i, i + 3)$ and $d_{\alpha N}(i, i + 3)$ NOE connectivities was observed and was important for confirmation of sequential assignments, as well as for establishing the location of the helix within the amino acid sequence. Few small $^3J_{HN\alpha}$ values could be resolved for these helices due to the large line widths of the NH resonances.

Sequential assignments for residues in the connecting loops and turns of the thioredoxin structure were also problematic, mainly as a result of rapid NH exchange and attenuation of COSY cross-peak intensity due to the small value of $^3J_{HN\alpha}$ often found in reverse turns. The loop or turn between Thr 8 and Ser 11 in both forms of thioredoxin posed particular difficulties. The C$^\alpha$H and C$^\beta$H resonances of the threonine are under the H_2O resonance and are nearly coincident, and the Asp 9 and Asp 10 NH resonances are nearly degenerate. The Asp 9 NH–C$^\alpha$H COSY cross peak is also highly attenuated. Ser 11 was sequentially assigned by using the d_{NN} NOE connectivity from Phe 12. The Asp 9 and Asp 10 NH resonances were identified by using NOE connectivities between the NH and C$^\beta$H resonances. Thr 8 and Asp 9 were connected by using a NOESY spectrum recorded at 328 K in which strong NOE connectivities are observed between the NH of Asp 9 and the C$^\alpha$H and C$^\beta$H resonances of Thr 8. Another difficult region was the sequence Asp 61–Thr 77, which not only contains a number of prolines but also appears to contain no regular secondary structure in either reduced or oxidized thioredoxin. Complete sequential assignment of these regions was obtained for both oxidation states by using a combination of $d_{\alpha N}$ and d_{NN} NOE connectivities.

The active-site region (C32–C35) is of particular interest, since the conformation in this region is likely to differ most significantly between the two forms of the protein. Sequential assignment of residues up to Trp 31 was straightforward. The NH of the Cys 32 residue can be identified from a distinctive d_{NN} NOE connectivity between Cys 32 and Trp 31 (circled in Figure 6). We experienced difficulty in assigning the Gly 33 resonances. No COSY or NOESY cross peaks could be observed for the NH proton of Gly 33 in the spectra of either oxidized or reduced thioredoxin at 308 K, and no remote peak at $\omega_2 = \omega_{NH}$, $\omega_1 = \omega_\alpha + \omega_{\alpha'}$ was observed in the 2Q spectrum. The C$^\alpha$H resonances of Gly 33 were assigned by elimination from the 2QF-COSY spectrum in ^2H_2O. For reduced thioredoxin, weak cross peaks between the C$^\alpha$H resonances and a resonance at 9.55 ppm were observed in the NOESY spectrum at 298 K. This NH resonance is not overlapped at this temperature, and a broad resonance at this chemical shift can be observed directly in a one-dimensional spectrum by using composite pulses instead of decoupling for solvent suppression. The assignment of this resonance to Gly 33 was confirmed by recording a NOESY spectrum using a composite pulse sequence for H_2O suppression (Figure 8). NOE connectivities are observed to the Gly 33 C$^\alpha$H protons and to the Pro 34 C$^\delta$H and Cys 32 C$^\alpha$H protons, establishing sequential connectivities for Gly 33 and Pro 34. Gly 33 was assigned for oxidized thioredoxin by using similar methods (Figure 8). The $d_{\alpha N}(i, i + 1)$ and $d_{\delta N}(i, i, + 1)$ connectivities between Pro 34 and Cys 35 are largely obscured by resonance overlap in NOESY spectra of reduced thioredoxin but are both clearly visible in NOESY spectra of oxidized thioredoxin. For reduced thioredoxin a weak $d_{\delta N}$ cross peak between Pro 34 and Cys 35 can be observed, partially overlapped with another peak

Table I: ^{1}H NMR Chemical Shifts of Reduced *E. coli* Thioredoxin (pH 5.7, T = 308 K)

residue	chemical shifts (ppm)					
	NH	$C^{\alpha}H$	$C^{\beta}H$	$C^{\gamma}H$	$C^{\delta}H$	other
Ser 1		4.19	3.90, 4.05			
Asp 2		4.73	2.78, 2.73			
Lys 3	8.35	4.30	1.91, 1.66	1.41, 1.50	1.67, 1.67	3.04, 3.04 ($C^{\epsilon}H$)
Ile 4	7.47	4.33	1.70	1.46, 0.89	0.66	0.47 ($C^{\gamma}H_3$)
Ile 5	8.41	4.20	1.72	1.15, 1.42	0.76	0.77 ($C^{\gamma}H_3$)
His 6	8.93	4.92	3.17, 3.17		7.20	8.19 ($C^{\epsilon}H$)
Leu 7	8.66	4.43	1.80, 1.33	1.46	0.67, 0.54	
Thr 8	8.03	4.76	4.73	1.30		
Asp 9	8.20	4.39	2.75, 2.80			
Asp 10	8.19	4.58	2.61, 2.69			
Ser 11	8.17	4.62	4.28, 3.67			
Phe 12	7.69	3.68	3.19, 3.30		7.06	6.95 ($C^{\epsilon}H$), 6.80 ($C^{\zeta}H$)
Asp 13	8.72	4.25	2.72, 2.79			
Thr 14	7.75	3.77	4.05	1.17		
Asp 15	8.37	4.26	2.27, 2.18			
Val 16	7.57	3.76	0.72	−0.13, −0.62		
Leu 17	6.96	3.87	2.38, 1.54	1.60	1.18, 0.89	
Lys 18	7.35	4.38	1.82, 2.10	1.45, 1.36	1.64, 1.59	2.98, 2.98 ($C^{\epsilon}H$)
Ala 19	6.61	4.22	1.27			
Asp 20	8.44	4.71	2.59, 2.68			
Gly 21	8.09	3.99, 3.99				
Ala 22	8.40	5.19	1.42			
Ile 23	8.97	5.13	1.71	1.06, 1.38	0.68	0.70 ($C^{\gamma}H_3$)
Leu 24	9.21	5.21	2.03, 1.27	1.45	0.96, 0.88	
Val 25	9.73	4.54	2.25	0.82, 0.26		
Asp 26	8.84	5.24	2.89, 2.23			
Phe 27	9.17	5.31	3.35, 2.75		7.36	7.04 ($C^{\epsilon}H$), 6.89 ($C^{\zeta}H$)
Trp 28	8.61	5.30	3.22, 3.08		7.25	10.70 ($N^{\epsilon}H$), 7.05 ($C^{\epsilon 3}H$), 6.97 ($C^{\zeta 3}H$), 7.33 ($C^{\eta}H$), 7.73 ($C^{\zeta 2}H$)
Ala 29	7.14	3.47	0.55			
Glu 30	9.04	4.11	2.07, 2.07	2.31, 2.39		
Trp 31	6.71	4.51	3.68, 3.21		7.47	11.37 ($N^{\epsilon}H$), 7.43 ($C^{\epsilon 3}H$), 7.19 ($C^{\zeta 3}H$), 7.23 ($C^{\eta}H$), 7.41 ($C^{\zeta 2}H$)
Cys 32	6.51	4.62	2.37, 1.67			
Gly 33	9.55[a]	3.98, 4.31				
Pro 34		4.41	2.43, 1.81	2.28, 2.03	3.73, 4.50	
Cys 35	7.81	4.09	3.29, 3.79			
Lys 36	7.82	4.09	2.08, 1.98	1.60, 1.52	1.81, 1.78	3.11, 2.99 ($C^{\epsilon}H$)
Met 37	7.62	4.25	2.20, 2.19	2.58, 2.68		2.08 ($C^{\epsilon}H_3$)
Ile 38	7.18	4.38	1.90	1.41, 1.43	0.81	1.05 ($C^{\gamma}H_3$)
Ala 39	7.17	3.82	1.34			
Pro 40		4.52	2.35, 1.95	2.02, 2.08	3.64, 3.83	
Ile 41	6.62	3.81	2.03	1.22, 1.71	0.98	0.86 ($C^{\gamma}H_3$)
Leu 42	7.90	3.83	1.87, 1.26	1.64	0.63, 0.63	
Asp 43	7.27	4.29	2.80, 2.68			
Glu 44	7.25	4.24	2.24, 2.07	2.62, 2.68		
Ile 45	8.50	3.96	2.15	1.31, 1.64	0.77	0.60 ($C^{\gamma}H_3$)
Ala 46	8.54	3.95	1.44			
Asp 47	7.12	4.55	2.84, 2.84			
Glu 48	8.51	4.03	2.00, 2.13	2.44, 2.44		
Tyr 49	8.68	4.38	2.80, 3.31		7.12	6.69 ($C^{\epsilon}H$)
Gln 50	7.08	4.33	2.36, 2.27	2.53, 2.50		
Gly 51	9.22	4.40, 3.74				
Lys 52	8.18	4.61	1.89, 1.95	1.43, 1.46	1.72, 1.66	2.94, 2.94 ($C^{\epsilon}H$)
Leu 53	7.85	4.78	1.79, 1.30	1.39	0.73, 0.50	
Thr 54	8.10	4.62	3.95	1.24		
Val 55	9.88	4.61	2.00	0.81, 0.85		
Ala 56	9.29	5.40	1.05			
Lys 57	8.65	5.10	1.97, 1.60	0.93, 1.26	2.08, 2.20	3.08, 3.08 ($C^{\epsilon}H$)
Leu 58	8.87	4.58	1.33, 0.93	1.30	0.93, 0.77	
Asn 59	9.01	4.01	2.65, 2.21			
Ile 60	8.60	4.22	2.19	1.40, 1.37	0.89	1.21 ($C^{\gamma}H_3$)
Asp 61	7.71	4.60	2.87, 2.70			
Gln 62	7.29	4.21	1.77, 2.20	2.28, 2.47		
Asn 63	7.36	5.18	2.72, 2.78			
Pro 64		4.73	2.36, 2.03	1.91, 1.98	3.38, 3.78	
Gly 65	10.20	3.98, 3.67				
Thr 66	7.87	3.80	3.75	0.45		
Ala 67	9.60	3.87	1.36			
Pro 68		4.35	1.75, 2.33	2.09, 1.97	3.48, 3.58	
Lys 69	7.38	3.87	1.82, 1.50	1.13, 1.13	1.60, 1.62	2.93, 2.93 ($C^{\epsilon}H$)
Tyr 70	7.30	4.41	3.39, 2.15		7.10	6.77 ($C^{\epsilon}H$)
Gly 71	7.50	3.82, 3.76				
Ile 72	7.08	3.78	1.55	0.75, 1.00	0.09	0.65 ($C^{\gamma}H_3$)
Arg 73	8.60	4.43	1.65, 1.90	1.52, 1.58	3.13, 3.13	7.14 ($N^{\epsilon}H$)
Gly 74	7.65	4.20, 3.74				
Ile 75	8.09	4.71	1.77	1.55, 1.09	0.41	0.77 ($C^{\gamma}H_3$)

Table I (Continued)

residue	chemical shifts (ppm)					
	NH	$C^{\alpha}H$	$C^{\beta}H$	$C^{\gamma}H$	$C^{\delta}H$	other
Pro 76		5.11	2.67, 2.03	1.65, 1.73	3.52, 3.58	
Thr 77	7.99	4.88	3.90	1.11		5.28 ($O^{\gamma}H$)
Leu 78	9.26	5.72	1.73, 1.20	1.74	0.81, 0.73	
Leu 79	9.07	5.10	1.87, 1.30	1.66	0.80, 0.86	
Leu 80	8.81	5.28	1.96, 1.03	1.30	0.72, 0.53	
Phe 81	9.93	5.18	2.95, 2.87		6.81	7.08 ($C^{\epsilon}H$), 6.40 ($C^{\zeta}H$)
Lys 82	8.79	4.60	1.61, 1.80	1.38, 1.25	1.68, 1.68	2.85, 2.85 ($C^{\epsilon}H$)
Asn 83	9.35	4.60	2.85, 3.11			
Gly 84	9.53	3.75, 4.38				
Glu 85	7.83	4.91	1.95, 2.11	2.32, 2.38		
Val 86	8.77	3.15	1.87	0.60, 0.57		
Ala 87	9.62	4.51	1.33			
Ala 88	7.66	4.61	1.36			
Thr 89	8.47	5.14	3.82	1.05		
Lys 90	8.99	4.47	1.21, 0.68	0.63, 0.70	1.48, 1.42	2.68, 2.62 ($C^{\epsilon}H$)
Val 91	8.54	4.57	1.91	0.82, 0.90		
Gly 92	8.24	3.59, 4.38				
Ala 93	8.16	3.98	1.36			
Leu 94	6.74	4.69	1.55, 1.61	1.71	0.67, 0.52	
Ser 95	8.33	4.58	4.31, 3.91			
Lys 96	9.27	3.80	1.95, 1.86	1.26, 1.26	1.68, 1.73	2.93, 2.93 ($C^{\epsilon}H$)
Gly 97	8.79	3.76, 3.92				
Gln 98	7.68	4.14	2.27, 1.93	2.45, 2.45		
Leu 99	8.53	4.10	1.90, 1.45	1.52	0.87, 0.74	
Lys 100	8.71	3.94	1.83, 1.99	1.50, 1.53	1.88, 1.78	3.08, 3.08 ($C^{\epsilon}H$)
Glu 101	7.80	4.06	2.15, 2.10	2.26, 2.45		
Phe 102	7.63	4.42	3.27, 3.33		7.15	6.99 ($C^{\epsilon}H$), 6.71 ($C^{\zeta}H$)
Leu 103	8.55	3.50	1.83, 0.92	1.86	0.60, 0.12	
Asp 104	9.17	4.35	2.70, 2.66			
Ala 105	7.50	4.22	1.44			
Asn 106	7.26	4.73	2.23, 1.88			
Leu 107	7.81	4.42	1.73, 1.65	1.76	0.84, 0.87	
Ala 108	7.47	4.09	1.35			

[a] 298 K.

The cis configuration of the Ile 75–Pro 76 peptide bond is evident from a $d_{\alpha\alpha}(i, i + 1)$ NOE connectivity (Arseniev et al., 1983; Wüthrich et al., 1984) between the two residues. The Ile 75–Pro 76 peptide bond appears to be entirely cis, and there is no indication of even a low population of the trans isomer: the $d_{\alpha\delta}$ or $d_{N\delta}$ NOE connectivities that would be expected for a trans peptide bond are absent for both oxidized and reduced thioredoxin.

Sequential assignment of Asp 2 was complicated for both forms of the protein by the lack of an obvious NH resonance for this amino acid. No evidence for the Asp 2 NH was apparent even in the NOESY spectrum obtained by using composite pulses for water suppression. This spectrum, however, showed a strong cross peak from a $C^{\alpha}H$ resonance at 4.73 ppm to the Lys 3 NH resonance in both forms of the protein. This assignment was confirmed by the observation of a $d_{\beta N}(i, i + 1)$ NOE connectivity between Asp 2 and Lys 3.

Discussion

We have been able to make sequence-specific resonance assignments for all backbone and side-chain protons of both oxidized and reduced thioredoxin from *E. coli*. Our assignment strategy (Chazin et al., 1987, 1988a) relies upon various forms of relayed coherence transfer and multiple quantum experiments to make amino acid spin system assignments followed by standard sequential assignment methods (Billeter et al., 1982). Sequential assignments of the NH, $C^{\alpha}H$, and some $C^{\beta}H$ resonances of oxidized thioredoxin have been reported previously (LeMaster & Richards, 1988). The backbone proton assignments are in agreement in the two independent studies, allowing for slight shifts due to differences in temperature and pH, the one exception being the $C^{\alpha}H$ resonance of Asp 9. Our present experiments show that the $C^{\alpha}H$–$C^{\beta}H_2$ spin system attributed to Asp 9 by LeMaster and Richards should, on the basis of several NOEs to Lys 3, be assigned to Asp 2. The Asp 2 spin system was not assigned in the earlier work. The assignments made for the $C^{\beta}H$ protons of Thr 8, Cys 32, Arg 73, Leu 78, Gln 98, Asn 106, and Leu 107 by LeMaster and Richards are in disagreement with ours. We note that, with the exception of Cys 32 where the cross peak is overlapped, our $C^{\beta}H_2$ assignments are supported by remote connectivities in double quantum spectra. The 3QF-COSY spectra were also particularly useful for assigning $C^{\beta}H$ and $C^{\beta\prime}H$ resonances, since both $C^{\alpha}H$–$C^{\beta}H$ cross peaks appear in this spectrum. Further confirmation of the chemical shifts of the $C^{\beta}H$ protons was provided by TOCSY spectra. We emphasize that our assignments are complete and self-consistent for both oxidized and reduced thioredoxin. The disagreements between our assignments and those of LeMaster and Richards (1988) appear to arise mainly from their failure to assign Asp 2 and the four proline $C^{\alpha}H$–$C^{\beta}H_2$ spin subsystems. The aromatic and aliphatic resonance assignments made by Hiraoki et al. (1988) on the basis of observed NOEs and distances estimated from the oxidized thioredoxin crystal structure are mostly in disagreement with our assignments.

The location of the elements of secondary and supersecondary structure and the overall topology of thioredoxin in solution can be deduced from the patterns of sequential, medium-range, and long-range NOE connectivities. Some small differences between the oxidized and reduced proteins are apparent and will be discussed below. The principal elements of secondary structure found in solution consist of a central β-sheet and three helices. The helices are located on the basis of sequential d_{NN} NOEs and networks of $d_{\alpha N}(i, i + 3)$ and $d_{\alpha\beta}(i, i + 3)$ NOE connectivities. In reduced thioredoxin, helix

Table II: ^{1}H NMR Chemical Shifts of Oxidized *E. coli* Thioredoxin (pH 5.7, T = 308 K)

residue	chemical shifts (ppm)					
	NH	$C^{\alpha}H$	$C^{\beta}H$	$C^{\gamma}H$	$C^{\delta}H$	other
Ser 1		4.19	4.06, 3.91			
Asp 2		4.72	2.77, 2.73			
Lys 3	8.34	4.29	1.92, 1.66	1.41, 1.49	1.66, 1.66	3.03, 3.03 ($C^{\epsilon}H$)
Ile 4	7.46	4.33	1.68	1.46, 0.89	0.63	0.46 ($C^{\gamma}H_3$)
Ile 5	8.38	4.21	1.73	1.14, 1.42	0.73	0.78 ($C^{\gamma}H_3$)
His 6	8.86	4.93	3.13, 3.19		7.21	8.20 ($C^{\epsilon}H$)
Leu 7	8.66	4.41	1.80, 1.33	1.46	0.66, 0.53	
Thr 8	8.08	4.77	4.74	1.30		
Asp 9	8.22	4.36	2.74, 2.78			
Asp 10	8.20	4.57	2.62, 2.68			
Ser 11	8.17	4.61	4.28, 3.69			
Phe 12	7.69	3.68	3.18, 3.30		7.07	6.94 ($C^{\epsilon}H$), 6.78 ($C^{\zeta}H$)
Asp 13	8.69	4.24	2.71, 2.78			
Thr 14	7.74	3.77	4.06	1.17		
Asp 15	8.38	4.25	2.25, 2.17			
Val 16	7.56	3.76	0.72	−0.14, −0.62		
Leu 17	6.96	3.87	2.36, 1.58	1.59	1.17, 0.88	
Lys 18	7.36	4.37	1.82, 2.09	1.45, 1.36	1.58, 1.64	2.96, 2.96 ($C^{\epsilon}H$)
Ala 19	6.60	4.21	1.27			
Asp 20	8.44	4.71	2.58, 2.66			
Gly 21	8.08	3.99, 3.99				
Ala 22	8.38	5.19	1.42			
Ile 23	8.96	5.13	1.73	1.06, 1.38	0.68	0.69 ($C^{\gamma}H_3$)
Leu 24	9.20	5.21	2.03, 1.26	1.42	0.96, 0.82	
Val 25	9.74	4.51	2.24	0.83, 0.26		
Asp 26	8.86	5.21	2.89, 2.20			
Phe 27	8.93	5.31	3.30, 2.75		7.36	7.05 ($C^{\epsilon}H$), 6.88 ($C^{\zeta}H$)
Trp 28	8.62	5.14	3.06, 2.93		7.19	10.71 ($N^{\epsilon}H$), 7.07 ($C^{\epsilon 3}H$, 6.93 ($C^{\zeta 3}H$), 7.32 ($C^{\eta}H$), 7.72 ($C^{\zeta 2}H$)
Ala 29	6.54	3.29	0.37			
Glu 30	9.28	4.16	2.07, 2.10	2.33, 2.36		
Trp 31	6.65	4.58	3.68, 3.19		7.44	11.53 ($N^{\epsilon}H$), 7.41 ($C^{\epsilon 3}H$), 7.15 ($C^{\zeta 3}H$), 7.21 ($C^{\eta}H$), 7.39 ($C^{\zeta 2}H$)
Cys 32	6.82	4.75	2.88, 3.18			
Gly 33	9.56[a]	4.04, 4.32				
Pro 34		4.46	2.52, 1.70	2.33, 2.10	3.89, 4.04	
Cys 35	8.21	4.41	4.34, 3.39			
Lys 36	7.92	4.07	2.12, 2.00	1.60, 1.60	1.80, 1.86	3.12, 3.10 ($C^{\epsilon}H$)
Met 37	7.61	4.27	2.24, 2.24	2.58, 2.70		2.08 ($C^{\epsilon}H_3$)
Ile 38	7.19	4.40	1.95	1.40, 1.42	0.80	1.08 ($C^{\gamma}H_3$)
Ala 39	7.18	3.83	1.35			
Pro 40		4.50	2.33, 1.92	2.03, 2.08	3.64, 3.82	
Ile 41	6.67	3.82	2.02	1.21, 1.69	0.98	0.86 ($C^{\gamma}H_3$)
Leu 42	7.88	3.82	1.90, 1.22	1.62	0.62, 0.62	
Asp 43	7.28	4.28	2.78, 2.68			
Glu 44	7.23	4.24	2.24, 2.07	2.62, 2.79		
Ile 45	8.49	3.95	2.15	1.31, 1.63	0.77	0.59 ($C^{\gamma}H_3$)
Ala 46	8.53	3.94	1.43			
Asp 47	7.12	4.55	2.83, 2.83			
Glu 48	8.51	4.02	2.00, 2.13	2.45, 2.45		
Tyr 49	8.69	4.38	3.30, 2.80		7.12	6.68 ($C^{\epsilon}H$)
Gln 50	7.08	4.33	2.36, 2.26	2.52, 2.48		
Gly 51	9.21	4.40, 3.73				
Lys 52	8.18	4.61	1.90, 1.98	1.44, 1.44	1.68, 1.64	2.93, 2.93 ($C^{\epsilon}H$)
Leu 53	7.85	4.78	1.29, 1.79	1.38	0.73, 0.49	
Thr 54	8.10	4.62	3.94	1.23		
Val 55	9.89	4.59	2.00	0.80, 0.86		
Ala 56	9.27	5.38	1.04			
Lys 57	8.65	5.11	1.59, 1.93	1.24, 0.90	2.06, 2.19	3.00, 3.00 ($C^{\epsilon}H$)
Leu 58	8.80	4.58	1.33, 0.90	1.31	0.93, 0.77	
Asn 59	9.01	4.01	2.68, 2.20			7.18, 5.50 ($N^{\delta}H$)
Ile 60	8.52	4.23	2.22	1.48, 1.40	0.93	1.23 ($C^{\gamma}H_3$)
Asp 61	7.77	4.60	2.89, 2.69			
Gln 62	7.17	4.20	1.75, 2.24	2.27, 2.44		
Asn 63	7.35	5.17	2.72, 2.80			
Pro 64		4.73	2.38, 2.07	1.97, 2.01	3.38, 3.78	
Gly 65	10.24	3.98, 3.65				
Thr 66	7.86	3.78	3.75	0.45		
Ala 67	9.67	3.87	1.33			
Pro 68		4.34	2.33, 1.75	1.98, 2.10	3.49, 3.57	
Lys 69	7.35	3.87	1.83, 1.50	1.11, 1.11	1.60, 1.60	2.91, 2.91 ($C^{\epsilon}H$)
Tyr 70	7.30	4.42	3.41, 2.17		7.11	6.76 ($C^{\epsilon}H$)
Gly 71	7.50	3.80, 3.75				
Ile 72	7.12	3.77	1.53	0.77, 0.96	0.08	0.60 ($C^{\gamma}H_3$)
Arg 73	8.54	4.41	1.64, 1.90	1.58, 1.53	3.14, 3.14	7.14 ($N^{\epsilon}H$)
Gly 74	7.66	4.25, 3.76				
Ile 75	8.21	4.73	1.92	1.54, 1.10	0.36	0.77 ($C^{\gamma}H_3$)

Table II (Continued)

residue	chemical shifts (ppm) NH	$C^{\alpha}H$	$C^{\beta}H$	$C^{\gamma}H$	$C^{\delta}H$	other
Pro 76		5.09	2.68, 2.04	1.65, 1.77	3.39, 3.68	
Thr 77	7.77	4.89	3.86	1.11		
Leu 78	9.26	5.73	1.70, 1.21	1.77	0.81, 0.73	
Leu 79	9.05	5.09	1.86, 1.37	1.66	0.83, 0.87	
Leu 80	8.83	5.29	1.95, 1.04	1.30	0.53, 0.73	
Phe 81	9.93	5.17	2.95, 2.85		6.80	7.07 ($C^{\epsilon}H$), 6.36 ($C^{\zeta}H$)
Lys 82	8.78	4.59	1.64, 1.80	1.38, 1.21	1.68, 1.68	2.85, 2.85 ($C^{\epsilon}H$)
Asn 83	9.34	4.59	2.85, 3.11			7.64, 6.88 ($N^{\delta}H$)
Gly 84	9.53	3.75, 4.37				
Glu 85	7.82	4.91	1.95, 2.09	2.34, 2.30		
Val 86	8.77	3.14	1.87	0.60, 0.56		
Ala 87	9.61	4.50	1.32			
Ala 88	7.67	4.60	1.35			
Thr 89	8.48	5.11	3.81	1.06		
Lys 90	8.99	4.49	1.23, 0.70	0.62, 0.72	1.49, 1.42	2.58, 2.64 ($C^{\epsilon}H$)
Val 91	8.57	4.57	1.93	0.86, 0.91		
Gly 92	8.10	3.63, 4.37				
Ala 93	8.14	3.97	1.36			
Leu 94	6.73	4.68	1.58, 1.58	1.71	0.68, 0.53	
Ser 95	8.34	4.60	4.33, 3.93			
Lys 96	9.28	3.80	1.95, 1.87	1.25, 1.25	1.70, 1.78	2.93, 2.93 ($C^{\epsilon}H$)
Gly 97	8.77	3.78, 3.92				
Gln 98	7.68	4.14	1.94, 2.29	2.44, 2.44		
Leu 99	8.52	4.10	1.90, 1.50	1.50	0.87, 0.74	
Lys 100	8.70	3.94	1.82, 2.00	1.50, 1.52	1.88, 1.81	3.11, 3.11 ($C^{\epsilon}H$)
Glu 101	7.81	4.05	2.10, 2.16	2.44, 2.44		
Phe 102	7.64	4.41	3.27, 3.33		7.15	6.99 ($C^{\epsilon}H$), 6.70 ($C^{\zeta}H$)
Leu 103	8.54	3.50	1.83, 0.94	1.86	0.60, 0.13	
Asp 104	9.17	4.35	2.73, 2.66			
Ala 105	7.51	4.21	1.43			
Asn 106	7.25	4.73	1.88, 2.23			
Leu 107	7.81	4.41	1.73, 1.61	1.75	0.84, 0.87	
Ala 108	7.47	4.08	1.35			

[a] 298 K.

1 extends between residues 11 and 19, helix 2 from Gly 33 in the active site to Tyr 49, and helix 3 between residues 96 and 107. The central β-sheet is well-defined by an extensive network of NOE connectivities between β-strands (Figure 9). The sheet is formed by residues 4–7 (strand β_1), 22–29 (β_2), 53–60 (β_3), 77–83 (β_4), and 88–92 (β_5). Strands β_1, β_3, and β_2 are aligned in a parallel sense, while β_2, β_4, and β_5 are antiparallel. Strands β_4 and β_5 are connected by a tight hairpin turn, and the NOE connectivities indicate a β-bulge at the N-terminal end of β_5 (residues 86 and 87). A detailed description of the conformation of this 7-residue β-bulge loop must await complete three-dimensional structure determination using distance geometry methods. The elements of secondary structure are summarized in Table III.

The helix between residues 11 and 19 in reduced thioredoxin in solution appears to be significantly distorted at residues Val 16 and Lys 18. For both of these residues $^3J_{HN\alpha}$ is larger than 9 Hz, indicating ϕ angles substantially different from those expected in a regular helix. Despite these distortions, the secondary structure still approximates that of a helix in this region, as evidenced by the network of $d_{\alpha N}(i, i+3)$ and $d_{\alpha\beta}(i, i+3)$ NOE connectivities. Significant $d_{\alpha N}(i, i+4)$ NOE connectivities are also present in this region. Helix 2 (residues 33–50) contains two prolines, Pro 34 and Pro 40. Pro 34 occurs in the first turn and is easily accommodated in the helix (Richardson, 1981). Although the present NMR studies do not indicate this directly, Pro 40 must disrupt the helical hydrogen bonding and distort the helix (Richardson, 1981).

Two reverse turns in reduced thioredoxin are clearly defined by the NMR data by using established criteria (Wüthrich et al., 1984; Wagner et al., 1986; Dyson et al., 1988b), including observation of a $d_{\alpha N}(i, i+2)$ NOE connectivity in particular. The observed coupling constants and NOE connectivities indicate a type II turn involving residues 49–52 and a type VI turn, with *cis*-Pro at position 3 of the turn, involving residues 74–77. This latter turn is probably of type VIb, in the terminology of Richardson (1981), since the $^3J_{HN\alpha}$ coupling constant at Ile 75 does not have the very small value that would be expected for a turn of type VIa (Dyson et al., 1988b). No other well-defined reverse turns are apparent from the NMR data. We note that the present NMR experiments show Pro

Table III: Location of β-Strands, Helices, and β-Turns

secondary structure	residues X-ray, oxidized[a]	NMR, oxidized	NMR, reduced
β-strands			
β_1	2–8	4–8[b]	4–8[b]
β_2	22–29	22–29	22–29
β_3	53–58	53–60	53–60
β_4	77–81	77–82	77–82
β_5	88–91	88–92	88–92
helix			
α_1	11–18	11–19	11/12–19
α_2	35–49	33–49	33–49
α_3	59–63		
α_4	95–107	96–107	96–108
3_{10}	66–70[c]	*d*	*d*
reverse turns			
1	8–11	*e*	*e*
2	32–35	*e*	*e*
3	49–52	49–52	49–52
4		74–77	74–77

[a] Holmgren et al. (1975). [b] Only residues 4–7 appear to form part of the β-sheet. [c] S. Katti, D. LeMaster, A. Holmgren, B.-O. Söderberg, and H. Eklund, unpublished observations. [d] The NOE connectivities indicate poorly defined helical or turnlike structures in this region in solution. [e] Resonance overlap precludes observation of any of the NOEs diagnostic of a β-turn.

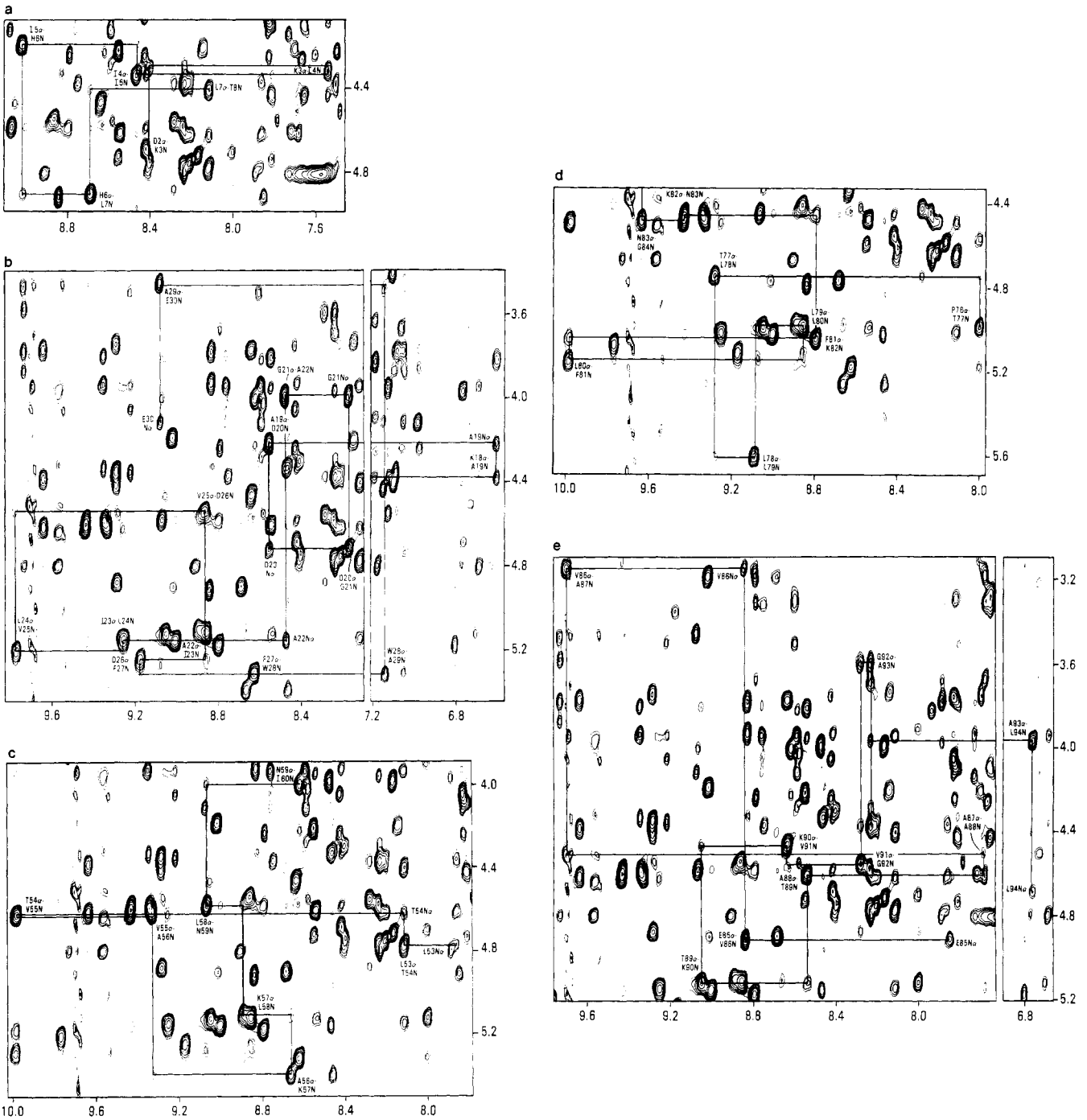

FIGURE 4: Portions of a 500-MHz phase-sensitive NOESY spectrum of reduced thioredoxin in 90% ^1H_2O/10% ^2H_2O, pH 5.70, 298 K, τ = 150 ms obtained by using a composite $45°_{(x)}$–τ–$45°_{(-x)}$ pulse sequence in place of the observe pulse (Clore & Gronenborn, 1983). NOE connectivities used to obtain sequential assignment of the β-strands are marked. (a) Strand 1 (Asp 2–Thr 8); (b) strand 2 (Lys 18–Glu 30); (c) strand 3 (Leu 53–Ile 60); (d) strand 4 (Thr 77–Asn 83); (e) strand 5 (Ala 88–Val 91) plus connectivities through the connecting loops Glu 85–Ala 87 and Gly 92–Lys 96.

76 to be exclusively cis in both oxidized and reduced thioredoxin, as indicated by an NOE connectivity between the $C^{\alpha}H$ of Ile 75 and the $C^{\alpha}H$ of Pro 76. No additional resonances were observed for protons in this part of the sequence, indicating that any population of thioredoxin with a *trans*-Pro 76 peptide bond is vanishingly small. Since isomerization of the Pro 76 peptide bond has been implicated in the rate-determining step of thioredoxin refolding (Kelley & Stellwagen, 1984), the observation that Pro 76 is exclusively cis in both oxidation states is important.

The constraints imposed by the secondary and supersecondary structure (Figure 9) allow a qualitative description of the global fold of reduced thioredoxin in solution. The folding topology is indicated schematically in Figure 10. The molecule consists of a central β-sheet comprising four long and one short β-strand with three helices packed against it. In qualitative terms, the overall fold of reduced thioredoxin in solution is, not surprisingly, very similar to that of oxidized thioredoxin in the crystalline state (Holmgren et al., 1975).

The NOE connectivities summarized in Figures 3, 5, and 8 show that the secondary structure, supersecondary structure, and folding topology of reduced and oxidized thioredoxin in solution are highly similar. The positions of the strands within the β-sheet are identical, as are the locations of the three helices. The well-defined reverse turns observed for reduced thioredoxin are retained in the oxidized protein. The apparent

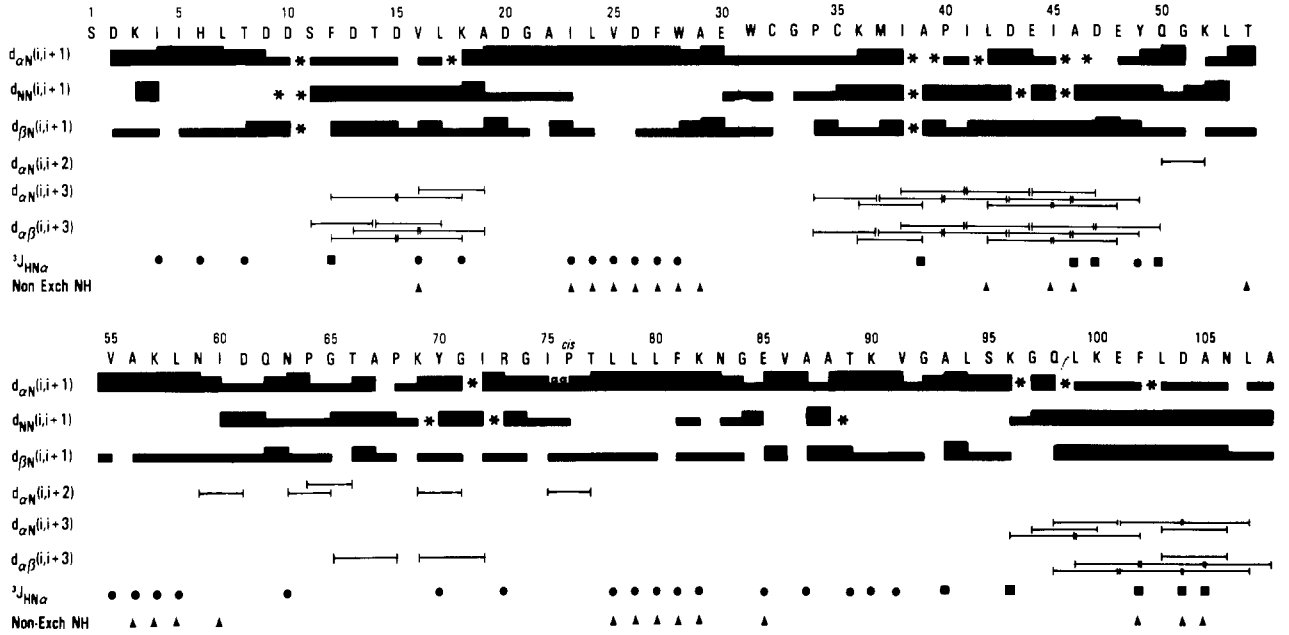

FIGURE 5: Summary of sequential connectivities for oxidized thioredoxin. The majority of the data were accumulated at 308 K, pH 5.7, but the diagram includes information from spectra obtained at other temperatures and pHs. Connectivities that were obscured by resonance overlap are labeled with an asterisk. Values of $^3J_{HN\alpha}$ are classified as small (≤6 Hz) or large (≥9 Hz) as indicated by solid squares and circles, respectively. Backbone amide protons that exchange slowly are indicated with a triangle. Note that $d_{\alpha\delta}$, $d_{N\delta}$, etc. connectivities for proline are included as $d_{\alpha N}$, d_{NN} connectivities. The $d_{\alpha\alpha}$ connectivity between Ile 75 and *cis*-Pro 76 is shown as a $d_{\alpha N}$ connectivity.

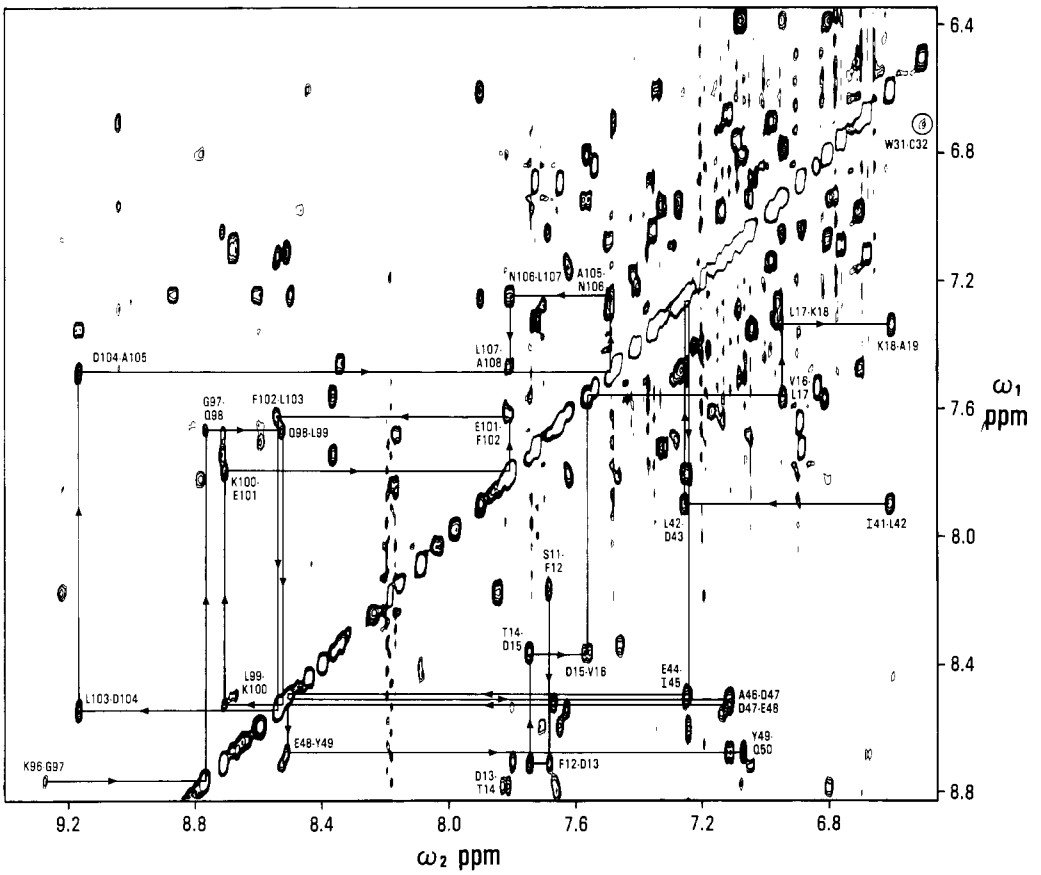

FIGURE 6: Portion of a 500-MHz phase-sensitive NOESY spectrum of reduced thioredoxin in 90% ^1H_2O/10% ^2H_2O, pH 5.70, 308 K, τ = 150 ms, showing $d_{NN}(i, i+1)$ connectivities in the helices. Helix 1 (Ser 11–Lys 18) and helix 2 (Ile 41–Gln 50) are shown below the diagonal; helix 3 (Lys 96–Ala 108) is shown above the diagonal.

differences in medium-range (i, $i+2$) and (i, $i+3$) NOE connectivities for residues 64–72 (Figures 3 and 5) probably do not reflect conformational differences between the oxidized and reduced proteins. Due to extensive resonance overlap for these resonances in one or both of the oxidation states, it is not clear whether NOEs are present or not. While the folded structures of oxidized and reduced thioredoxin are highly similar, subtle conformational differences clearly exist, as evidenced by the significant chemical shift differences for protons of residues in and near the active site (Tables I and

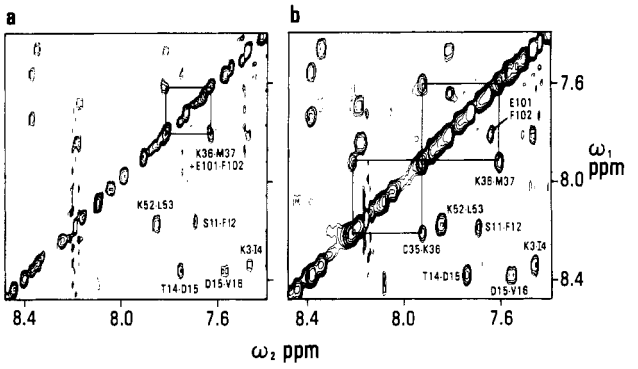

FIGURE 7: Portion of a 500-MHz phase-sensitive NOESY spectrum, showing part of the amide diagonal region, for (a) reduced thioredoxin and (b) oxidized thioredoxin. These spectra were obtained under identical conditions, pH 5.70 in 90% ^1H_2O/10% ^2H_2O, 308 K, τ = 150 ms.

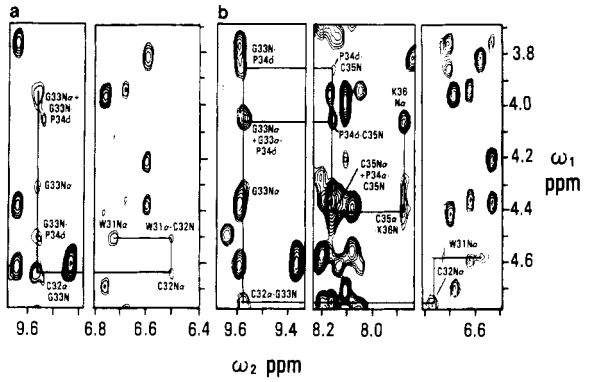

FIGURE 8: (a) Portion of the same spectrum as in Figure 4, showing the connectivities in the active site of reduced thioredoxin (Cys 32–Lys 36). (b) Portion of a NOESY spectrum obtained under identical conditions for oxidized thioredoxin, showing connectivities in the active-site region.

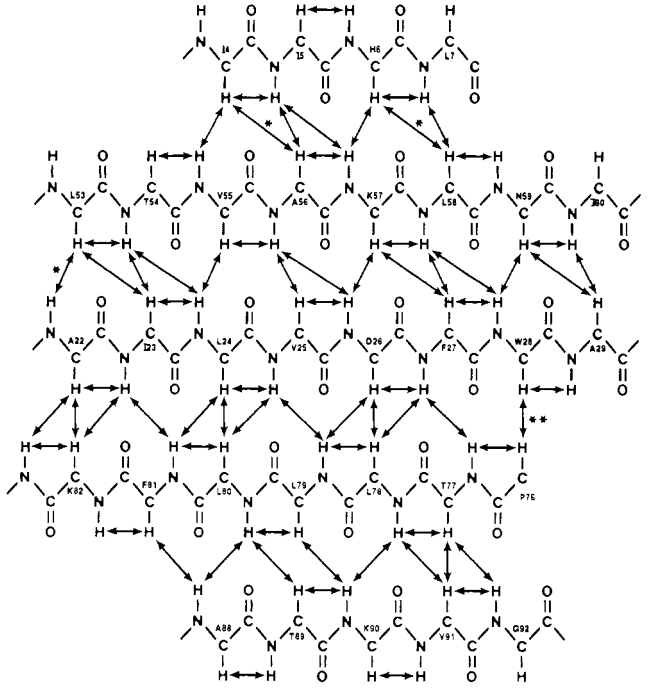

FIGURE 9: Supersecondary structure of oxidized and reduced *E. coli* thioredoxin, showing connections between the five strands of the central β-sheet. A single asterisk indicates NOE connectivities visible in the spectra of oxidized thioredoxin only. Double asterisks indicate an NOE connectivity visible in the spectra of reduced thioredoxin but overlapped in the spectrum of oxidized thioredoxin.

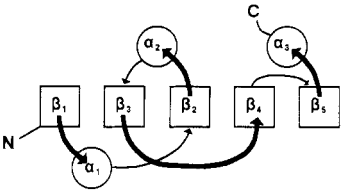

FIGURE 10: Schematic representation of the topology and packing of β-strands and helices in oxidized and reduced thioredoxin, viewed down the axis of the β-sheet. Boxes indicate β-strands, circles indicate α-helices, curved thick lines indicate loops above the β-sheet, and curved thin lines indicate loops below the β-sheet. Crossover connections between β-strands are right-handed, in accordance with the predominant handedness seen in protein structures (Richardson, 1981) and the NOEs observed between the helices and the β-sheet.

II; Dyson et al., 1988a). With the exception of differences in NOEs between the side chains of Trp 28, Ala 29, and Asn 59, there are no obvious differences in the pattern of NOE connectivities between the two oxidation states. It appears that the backbone conformations are highly similar, even in the active site itself, and that the observed chemical shift differences may involve changes in side-chain conformation or subtle changes in hydrogen bonding. A detailed description of the structural and dynamic differences between oxidized and reduced thioredoxin, which are clearly manifest in their different biochemical behavior, must await refinement of the solution structures at present being determined in this laboratory by using distance geometry and restrained molecular dynamics methods.

While it is clear from the NMR data that the overall fold of oxidized thioredoxin is the same in solution and in the crystalline state (Holmgren et al., 1975), subtle differences in local structure are observed. The locations of the regular elements of secondary structure in crystal and solution are compared in Table III. The most notable difference is the apparent absence in solution of a short helix found between residues 59 and 63 in the crystal structure. With the exception of an extremely weak $d_{\alpha N}(i, i + 3)$ NOE between Asn 59 and Gln 62 in the reduced thioredoxin, neither the characteristic NOE connectivities nor the small $^3J_{HN\alpha}$ coupling constants expected for a stretch of α-helix are observed experimentally. Indeed, the strongest medium-range NOE connectivity observed in this region is between the Asn 59 C$^\alpha$H and the Asp 61 NH protons, suggesting that the structure in solution is more like a reverse turn. The first β-strand does not appear to extend as far in solution as in the crystalline state (Table III), with a strong d_{NN} NOE connectivity between Lys 3 and Ile 4 clearly signaling deviations from β-structure. We note that one of the Cu^{2+} ions necessary for crystallization (Holmgren et al., 1975) is coordinated to Asp 2 and may explain the apparent conformational differences in this region. More detailed comparison of the crystal and solution structures must await completion of the three-dimensional solution structure.

In summary, the present NMR studies show that the overall structure of oxidized thioredoxin is very similar in the crystal and solution states. The present studies further serve to stress the overall structural similarity of oxidized and reduced thioredoxin. The conformational differences between these forms are clearly very subtle and are reflected in changes in chemical shifts of residues in and around the active site (Tables I and II; Dyson et al., 1988a) rather than in obvious changes in patterns of NOE connectivities. Determination of the nature of these conformational differences thus poses an interesting challenge to our present methods of solution structure determination based on semiquantitative evaluation of NOE in-

tensities to provide conservative distance constraints.

Acknowledgments

We thank Linda Tennant and Pia Lundman for expert technical assistance, Lonnie Harvey, Jerri Columpus, and Kathy Carpenter for assistance in preparation of the manuscript, and Drs. Mark Rance and Walter Chazin for helpful discussions.

Supplementary Material Available

A more detailed description of the spin system and sequential assignment procedure for residues that were problematic in either reduced or oxidized thioredoxin, together with a table summarizing the spectroscopic evidence for scalar connectivities within spin systems for reduced thioredoxin and figures showing the NH–C$^{\alpha}$H fingerprint region of the 2Q spectrum and the sequential NOE connectivities for oxidized thioredoxin (14 pages). Ordering information is given on any current masthead page.

References

Arseniev, A. S., Kondakov, V. I., Maiorov, V. N., Volkova, T. M., Grishin, E. V., Bystrov, V. F., & Ovchinnikov, Y. A. (1983) *Bioorg. Khim. 9*, 768–793.

Bax, A., & Davis, D. G. (1985) *J. Magn. Reson. 65*, 355–360.

Billeter, M., Braun, W., & Wüthrich, K. (1982) *J. Mol. Biol. 155*, 321–346.

Braunschweiler, L., Bodenhausen, G., & Ernst, R. R. (1983) *Mol. Phys. 48*, 535–560.

Chazin, W. J., & Wright, P. E. (1987) *Biopolymers 26*, 973–977.

Chazin, W. J., & Wüthrich, K. (1987) *J. Magn. Reson. 72*, 358–363.

Chazin, W. J., & Wright, P. E. (1988) *J. Mol. Biol. 202*, 623–636.

Chazin, W. J., Rance, M., & Wright, P. E. (1987) *FEBS Lett. 222*, 109–114.

Chazin, W. J., Rance, M., & Wright, P. E. (1988a) *J. Mol. Biol. 202*, 603–622.

Chazin, W. J., Hugli, T., & Wright, P. E. (1988b) *Biochemistry 27*, 9139–9148.

Clore, G. M., & Gronenborn, A. M. (1983) *J. Magn. Reson. 53*, 423–426.

Drobny, C., Pines, A., Sinton, S., Weitekamp, D., & Wemmer, D. (1979) *Symp. Faraday Soc. 13*, 49–55.

Dyson, H. J., Holmgren, A., & Wright, P. E. (1988a) *FEBS Lett. 228*, 254–258.

Dyson, H. J., Rance, M., Houghten, R. A., Lerner, R. A., & Wright, P. E. (1988b) *J. Mol. Biol. 201*, 161–200.

Eich, G., Bodenhausen, G., & Ernst, R. R. (1982) *J. Am. Chem. Soc. 104*, 3731–3732.

Eklund, H., Cambillau, C. Sjöberg, B.-M., Holmgren, A., Jörnvall, H., Höög, J.-O., & Brändén, C.-I. (1984) *EMBO J. 3*, 1443–1449.

Gleason, F. K., & Holmgren, A. (1988) *FEMS Microbiol. Rev. 54*, 271–298.

Hiraoki, T., Brown, S. B., Stevenson, K. J., & Vogel, H. J. (1988) *Biochemistry 27*, 5000–5008.

Holmgren, A. (1968) *Eur. J. Biochem. 6*, 475–484.

Holmgren, A. (1972) *J. Biol. Chem. 247*, 1992–1998.

Holmgren, A. (1985) *Annu. Rev. Biochem. 54*, 237–271.

Holmgren, A., & Reichard, P. (1967) *Eur. J. Biochem. 2*, 187–196.

Holmgren, A., & Roberts, G. (1976) *FEBS Lett. 71*, 261–265.

Holmgren, A., Söderberg, B.-O., Eklund, H., & Brändén, C.-I. (1975) *Proc. Natl. Acad. Sci. U.S.A. 72*, 2305–2309.

Höög, J.-O., von Bahr-Lindstrom, H., Josephson, S., Wallace, B. J., Kushner, S., Jörnvall, H., & Holmgren, A. (1984) *Biosci. Rep. 4*, 917–923.

Huber, H. E., Russel, M., Model, P., & Richardson, C. C. (1986) *J. Biol. Chem. 261*, 15006–15012.

Jeener, J., Meier, B. H., Bachmann, P., & Ernst, R. R. (1979) *J. Chem. Phys. 71*, 4546–4553.

Kelley, R. F., & Stellwagen, E. (1984) *Biochemistry 23*, 5095–5102.

LeMaster, D. M., & Richards, F. M. (1988) *Biochemistry 27*, 142–150.

Lim, C.-J., Geraghty, D., & Fuchs, J. A. (1985) *J. Bacteriol. 163*, 311–316.

Lunn, C. A., Kathju, S., Wallace, B. J., Kushner, S. R., & Pigiet, V. (1984) *J. Biol. Chem. 259*, 10469–10474.

Marion, D., & Wüthrich, K. (1983) *Biochem. Biophys. Res. Commun. 113*, 967–974.

Mark, D. F., & Richardson, C. C. (1976) *Proc. Natl. Acad. Sci. U.S.A. 73*, 780–784.

Neuhaus, D., Wagner, G., Vâsak, M., Kägi, J. H. R., & Wüthrich, K. (1985) *Eur. J. Biochem. 151*, 257–273.

Otting, E., Widmer, H., Wagner, G., & Wüthrich, K. (1986) *J. Magn. Reson. 66*, 187–193.

Rance, M. (1987) *J. Magn. Reson. 74*, 557–564.

Rance, M., & Wright, P. E. (1986) *J. Magn. Reson. 66*, 372–378.

Rance, M., Sørensen, O. W., Bodenhausen, G., Wagner, G., Ernst, R. R., & Wüthrich, K. (1983) *Biochem. Biophys. Res. Commun. 117*, 479–485.

Rance, M., Chazin, W., Dalvit, C., & Wright, P. E. (1989) *Methods Enzymol. 176*, 114–134.

Richardson, J. S. (1981) *Adv. Protein Chem. 34*, 167–339.

Russel, M., & Model, P. (1985) *Proc. Natl. Acad. Sci. U.S.A. 82*, 29–33.

Russel, M., & Model, P. (1986) *J. Biol. Chem. 261*, 14997–15005.

Stryer, L., Holmgren, A., & Reichard, P. (1967) *Biochemistry 6*, 1016–1020.

Wagner, G., Neuhaus, D., Wörgötter, E., Vâsak, M., Kägi, J. H. R., & Wüthrich, K. (1986) *J. Mol. Biol. 187*, 131–135.

Wüthrich, K., Billeter, M., & Braun, W. (1984) *J. Mol. Biol. 180*, 715–740.